

Q²SAR: A Quantum Multiple Kernel Learning Approach for Drug Discovery

Alejandro Giraldo  Daniel Ruiz  Mariano Caruso  Javier Mancilla  Guido Bellomo 
QNOW Technologies QNOW Technologies UGR, Granada, Spain Falcondale LLC CONICET - UBA
Delaware, USA Delaware, USA UNIR, La Rioja, Spain Delaware, USA ICC, Argentina
alejandro@qnow.tech daniel@qnow.tech FIDESOL, Granada, Spain javier@falcondale.pro gbellomo@icc.fcen.uba.ar
mcaruso@fidesol.org

Abstract—Quantitative Structure-Activity Relationship (QSAR) modeling is a cornerstone of computational drug discovery. This research demonstrates the successful application of a Quantum Multiple Kernel Learning (QMKL) framework to enhance QSAR classification, showing a notable performance improvement over classical methods. We apply this methodology to a dataset for identifying DYRK1A kinase inhibitors. The workflow involves converting SMILES representations into numerical molecular descriptors, reducing dimensionality via Principal Component Analysis (PCA), and employing a Support Vector Machine (SVM) trained on an optimized combination of multiple quantum and classical kernels. By benchmarking the QMKL-SVM against a classical Gradient Boosting model, we show that the quantum-enhanced approach achieves a superior AUC score, highlighting its potential to provide a quantum advantage in challenging cheminformatics classification tasks.

Index Terms—QSAR, classification, drug discovery, quantum machine learning, multiple kernel learning, support vector machines.

I. INTRODUCTION

II. QSAR THEORY AND CONTEMPORARY RELEVANCE

A. Foundations of Quantitative Structure-Activity Relationships

Quantitative Structure-Activity Relationship (QSAR) modeling represents a cornerstone (one of them) methodology in computational chemistry and drug discovery, embodying the fundamental principle that molecular structure can determine biological activity. This paradigm, first conceptualized by Hansch and Fujita in the 1960s, has evolved into a sophisticated computational framework that bridges chemical structure and pharmacological function through mathematical modeling [1].

QSAR models are statistical tools that relate molecular descriptors to a property of interest, such as physicochemical, toxicological, or biological activity. Typically, these models are constructed using machine learning (ML) algorithms. The general workflow for developing QSAR models has been extensively documented [2] [3].

Similar to SAR (Structure-Activity Relationship) analysis, QSAR modeling requires a dataset of molecules with well-defined structures and experimentally determined activities. Molecular descriptors—numerical representations of molecular characteristics—are calculated for each compound. These descriptors can include atom counts (e.g., number

of heteroatoms), fragment counts (e.g., number of benzene rings), topological indices (describing the molecule’s connectivity), and 3D descriptors (capturing spatial features of the molecules). [4]

The theoretical foundation of QSAR rests on the premise that similar molecular structures exhibit similar biological activities—a principle that enables the systematic prediction of pharmacological, toxicological, and physicochemical properties from structural information alone. In essence, QSAR transforms the complex relationship between molecular architecture and biological response into a tractable computational problem through the systematic encoding of chemical structures into numerical descriptors [5].

Structurally, QSAR models function as statistical or machine learning frameworks that utilize molecular descriptors as predictor variables for properties of interest, whether physicochemical (solubility, lipophilicity), biological (enzyme inhibition, receptor binding), or toxicological (mutagenicity, carcinogenicity). The general QSAR workflow encompasses molecular representation via SMILES strings, descriptor calculation, feature engineering, model development, and validation—a pipeline that has become increasingly sophisticated with advances in cheminformatics and machine learning.

B. Contemporary Relevance and Industrial Impact

The relevance of QSAR methodologies in modern drug discovery has intensified dramatically due to several converging factors that define the current pharmaceutical landscape. The exponential growth in chemical databases, with repositories like ChEMBL and PubChem containing millions of bioactive compounds, necessitates computational approaches capable of rapid property prediction and compound prioritization.

Three fundamental advantages position QSAR as an indispensable tool in contemporary drug development:

(i) **Predictive Efficiency:** Once developed and validated, QSAR models enable instantaneous property prediction from molecular structure alone, eliminating the need for costly and time-intensive experimental screening. This capability is particularly valuable in early-stage drug discovery, where rapid assessment of large compound libraries is essential for lead identification and optimization.

(ii) Scalability and Automation: Modern QSAR frameworks support fully automated evaluation of massive chemical spaces, facilitating the assessment of millions of virtual compounds through high-throughput computational screening. This scalability aligns with current trends toward big data approaches in pharmaceutical research, where comprehensive exploration of chemical space is increasingly feasible.

(iii) Regulatory Acceptance: QSAR models have achieved widespread acceptance by regulatory agencies, including the OECD, EPA, and EMA, particularly for toxicity assessment and environmental risk evaluation. This regulatory validation ensures that QSAR-based predictions can support formal safety assessments and regulatory submissions, providing a pathway from computational prediction to clinical application.

C. Machine Learning Enhancement and Quantum Frontiers

The integration of advanced machine learning algorithms into QSAR workflows has revolutionized the field’s predictive capabilities, enabling the capture of complex, non-linear structure-activity relationships that were previously intractable. Deep learning architectures, ensemble methods, and sophisticated feature selection algorithms have expanded QSAR’s applicability to increasingly challenging molecular targets and property predictions.

However, as chemical datasets grow in complexity and dimensionality, traditional computational approaches encounter fundamental limitations in feature space exploration and pattern recognition. This challenge motivates the exploration of quantum machine learning approaches, which leverage the exponentially large Hilbert spaces of quantum systems [6], to potentially identify molecular patterns that remain hidden to classical algorithms.

The emergence of Quantum Machine Learning (QML) in cheminformatics represents a paradigm shift toward harnessing quantum computational principles for enhanced molecular property prediction.

By mapping classical molecular data into quantum states through specialized feature maps, quantum algorithms can potentially access richer representational spaces and capture subtle structure-activity relationships that classical methods might overlook [7].

Quantitative Structure-Activity Relationship (QSAR) models aim to establish a quantitative link between the chemical structure of a molecule and its biological activity [8]. These mathematical models provide an *in silico* methodology to predict the properties of novel compounds, thereby prioritizing experimental efforts and reducing costs. Applications range from predicting pharmacokinetic processes—absorption, distribution, metabolism, and excretion (ADME)—to assessing toxicological endpoints, and even modelling new properties.

The evolution of QSAR has seen a shift from simple linear regression to more sophisticated machine learning algorithms. Methods like Random Forests [9] and Bayesian Neural Networks [10] have shown superior performance by capturing complex, non-linear relationships within the data. However, as molecular data grows in complexity, in the sense its important

to describe our compound in more ways than just than a few feature our dataset that captures all this relations growths also in complexity. There is an ongoing need for methods that can effectively navigate high-dimensional feature spaces.

Quantum Machine Learning (QML) offers a promising new direction. By mapping classical data into the exponentially large Hilbert spaces of quantum systems, QML algorithms, particularly Quantum Support Vector Machines (QSVMs) [11], have the potential to identify patterns that are intractable for classical models [12]. This work focuses on a specific enhancement of QSVMs known as Quantum Multiple Kernel Learning (QMKL) [13], where we combine the strengths of various quantum and classical kernels to build a more robust and accurate classifier for a real-world drug discovery problem.

III. METHODOLOGY

Our pipeline consists of three main stages: **(1)** data preprocessing and feature engineering, **(2)** classification using a QMKL-SVM model, and **(3)** benchmarking against a classical Gradient Boosting model.

QSAR models are evaluated using various metrics that assess predictive performance [4]. Key metrics include:

- **Accuracy (ACC)**
- **Precision (PPV)**
- **Sensitivity (Recall, TPR)**
- **Specificity (TNR)**
- **F1-score**
- **Matthews Correlation Coefficient (MCC)**

In our research, we use the **ROC-AUC** as a key metric to benchmark classical and quantum pipelines, as mentioned in the corresponding section.

A. Dataset Description and Preprocessing

This study is based on a high-quality dataset provided and curated by the team at [ProtoQSAR SL](#), their contribution was fundamental in the selection of compounds, the calculation, and validation of molecular descriptors.

This dataset serves as the foundational benchmark for developing our quantum machine learning model. By establishing a consistent baseline, it enables robust comparisons and benchmarking against other models trained on the same data.

The dataset was compiled from public dataset of DYRK1A (Dual-specificity tyrosine-phosphorylation-regulated kinase 1A) inhibitors [14]. A comprehensive dataset of 1291 molecules exhibiting inhibitory activity against human DYRK1A kinase was systematically compiled from the ChEMBL database (ChEMBLID : ChEMBL2292). DYRK1A represents a critical therapeutic target for neurodegenerative disorders, particularly Alzheimer’s disease, due to its role in tau phosphorylation and neuronal dysfunction [15].

The kinase’s involvement in Down syndrome-associated cognitive impairment and its potential as a druggable target for neuroprotective interventions makes it an ideal case study for quantum-enhanced QSAR modeling approaches.

The raw dataset underwent rigorous quality control procedures to ensure data integrity and experimental consistency. The curation pipeline comprised three critical stages: (i) identification and removal of duplicate molecular entries, (ii) validation of chemical structures to eliminate invalid SMILES representations, and (iii) application of bioassay selection criteria. Specifically, only compounds from experiments annotated with BioAssay Ontology (BAO) label "single protein assay" were retained to ensure direct target-compound interaction measurements, excluding complex cellular or multi-target assays that could introduce confounding factors.

Following systematic curation, the final data set comprised 354 unique molecules with experimentally determined IC_{50} values that ranged from 0.5 nM to 100 μM . For binary classification, compounds were categorized using a standard medicinal chemistry threshold established for kinase inhibitors: molecules with $pIC_{50} \geq 6.0$ (corresponding to $IC_{50} \leq \mu M$) were classified as "active" inhibitors, while those below this threshold were designated as "inactive". [4].

1) *Molecular Descriptors*: The feature set comprised representative molecular descriptors from established cheminformatics libraries (RDKit, Mordred).

a) *Shape and Geometric Descriptors*: **PMI1** (Principal Moment of Inertia, 1st order): The first principal moment of inertia calculated from the 3D molecular coordinates, representing the distribution of atomic masses around the principal axis. PMI1 values typically range from 10 to 1000 $amu \cdot \text{\AA}^2$ for drug-like molecules, with higher values indicating more elongated structures.

NPR1 (Normalized Principal Ratio 1): The ratio $PMI1/PMI3$, normalized to eliminate molecular size effects. NPR1 values range from 0.5 (spherical) to 1.0 (linear), providing size-independent shape characterization essential for scaffold-hopping applications.

b) *Electronic and Topological Descriptors*: **MolLogP** (Molecular LogP): Octanol-water partition coefficient calculated using the Wildman-Crippen method implemented in RDKit. Values typically range from -3 to +8 for drug-like compounds, with optimal range 1-3 for oral bioavailability.

TPSA (Topological Polar Surface Area): Sum of surfaces of polar atoms (oxygen and nitrogen) in a molecule, calculated using group contributions. TPSA values $< 140 \text{\AA}^2$ correlate with good blood-brain barrier permeability.

NumRotatableBonds: Count of rotatable bonds in the molecule, excluding amide bonds. Drug-like molecules typically have ≤ 10 rotatable bonds according to Lipinski's rule.

c) *Connectivity and Graph-Based Descriptors*: **BertzCT** (Bertz Complexity Index): A graph-theoretical descriptor that quantifies molecular complexity by considering both the number of atoms and their connectivity patterns. Typical values range from 0 for simple molecules (e.g., methane) to over 1000 for complex natural products [16]. It considers both the number of atoms and their connectivity patterns within a molecular structure. This index helps in understanding and predicting the complexity of molecules, particularly in the context of synthetic planning and analysis of synthetic

strategies. The Bertz Complexity Index utilizes graph theory to represent molecules. In this representation, atoms are nodes (vertices) and bonds are edges within the graph.

Chi0n, Chi1n (Kier-Hall Connectivity Indices): Topological indices describing molecular branching and connectivity. Chi0n reflects molecular size, while Chi1n captures first-order connectivity patterns.

d) *Pharmacophore and Functional Group Descriptors*:

NumHBD (Hydrogen Bond Donors): Count of hydrogen bond donor groups (OH, NH). Drug-like molecules typically have ≤ 5 donors.

NumHBA (Hydrogen Bond Acceptors): Count of hydrogen bond acceptor atoms (N, O). Optimal range ≤ 10 for oral drugs.

FractionCsp3: Fraction of carbons that are sp^3 hybridized. Higher Fsp3 values (> 0.47) correlate with increased three-dimensionality and improved developability.

NumAromaticRings: Count of aromatic ring systems in the molecule. Excessive aromatic content (> 4 rings) often correlates with poor solubility and toxicity issues.

e) *Validation and Quality Control*: All descriptors were calculated using RDKit 2023.03.1 with default parameters and validated against reference compounds from the ChEMBL database. Descriptor values were checked for reasonable ranges based on drug-like chemical space: molecular weight (150-500 Da), LogP (-2 to 5), TPSA (20-140 \AA^2), and rotatable bonds (0-10). This validation ensures that the quantum feature mapping operates on chemically meaningful and computationally stable molecular representations.

This high-dimensional descriptor matrix provides a comprehensive mathematical representation of molecular structure, capturing diverse aspects of chemical information essential for robust QSAR model development.

The dataset is pre-divided into a training set and a test set, with each compound labeled with a binary target, $y \in \{0, 1\}$, indicating its inhibitory activity.

A multi-step preprocessing pipeline was implemented to prepare the data for our models:

- 1) **Numerical Feature Extraction**: The primary molecular structure is given as a SMILES (Simplified Molecular Input Line Entry System) string. As machine learning models require numerical input, we used the RDKit library to convert each SMILES string into a high-dimensional vector of approximately 200 physicochemical descriptors (e.g., molecular weight, LogP, topological polar surface area).
- 2) **Standardization**: The resulting numerical feature set was standardized using Scikit-learn's `StandardScaler`, which scales each feature to have a mean of 0 and a standard deviation of 1. The scaler was fitted only on the training data to prevent data leakage.
- 3) **Dimensionality Reduction**: To create a feature set suitable for current quantum hardware and simulators, PCA was applied. We reduced the high-dimensional descriptor space to $n = 4$ principal components, which capture the maximum variance in the data. These four

components serve as the final input features for all subsequent models.

B. Quantum Multiple Kernel Learning

Support Vector Machines (SVM) are powerful classifiers that work by finding an optimal hyperplane separating data points in a high-dimensional feature space. The "kernel trick" allows SVMs to operate in this space implicitly, without ever computing the coordinates of the data in that space. A kernel function, $K(\mathbf{x}_i, \mathbf{x}_j)$, computes the similarity between two data points \mathbf{x}_i and \mathbf{x}_j .

Our approach extends this concept by using Quantum Multiple Kernel Learning [13].

1) *Quantum Kernels*: A quantum kernel, \mathcal{K} , is created by first encoding classical data points \mathbf{x} into quantum states $|\psi(\mathbf{x})\rangle$ via a quantum feature map, which is a parameterized quantum circuit $U(\mathbf{x})$ [17]. The kernel value is then the similarity measure between these two quantum states, typically the fidelity:

$$\mathcal{K}(\mathbf{x}_i, \mathbf{x}_j) = |\langle \psi(\mathbf{x}_i) | \psi(\mathbf{x}_j) \rangle|^2 = |\langle 0 | U^\dagger(\mathbf{x}_i) U(\mathbf{x}_j) | 0 \rangle|^2. \quad (1)$$

This process leverages quantum properties like superposition and entanglement to potentially map the data into a richer feature space [18]. We used a feature map composed of angle-embedding rotations and CNOT entangling gates [19].

2) *Kernel combination*: Instead of relying on a single kernel, MKL seeks to find the best possible linear combination of a pre-defined set of basis kernels $\{K_i\}_{i=1, \dots, m}$ given by

$$K = \sum_{i=1}^m w_i K_i, \quad \text{with } w_i \geq 0, \quad \sum_{i=1}^m w_i = 1. \quad (2)$$

In our work, the set of basis kernels included several different quantum fidelity kernels (generated by varying the feature map parameters) and a classical Radial Basis Function (RBF) kernel. The optimal weights w_i were determined using an average alignment, which maximizes the similarity between the combined kernel and an ideal target kernel derived from the training labels.

C. Classical Benchmark Model

A classical GradientBoostingClassifier from Scikit-learn was trained and evaluated on the exact same 4-dimensional, PCA-processed data. This ensures a fair and direct comparison of the classification power of the QMKL – SVM against a strong, widely-used classical algorithm.

IV. RESULTS AND DISCUSSION

The performance of both the final QMKL – SVM model and the classical Gradient Boosting model was evaluated on the unseen test set. The primary metric for comparison is the Area Under the Receiver Operating Characteristic Curve (ROC – AUC).

Table I summarizes the final performance scores. The QMKL – SVM model achieved an AUC of **0.8750**, demonstrating a clear and significant performance improvement over the

classical Gradient Boosting model, which scored an AUC of **0.8037**. This result highlights the effectiveness of the quantum kernel-based approach for this classification task.

TABLE I
PERFORMANCE COMPARISON ON THE DYRK1A TEST SET

Model	ROC-AUC Score
QMKL-SVM	0.8750
Gradient Boosting	0.8037

Figure 1 provides a visual comparison of the ROC curves for both models. The plot clearly illustrates the superior performance of the QMKL – SVM, as its curve consistently stays above the Gradient Boosting curve, thereby encompassing a larger area. Both models perform significantly better than a random classifier, but the quantum-enhanced model shows a distinct advantage in its ability to separate the active and inactive compounds.

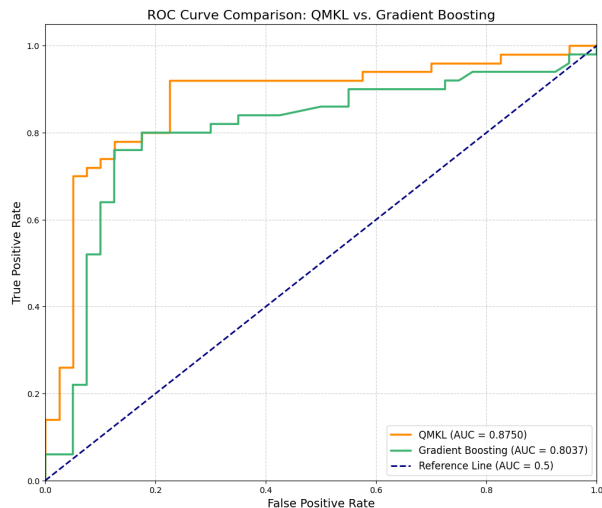


Fig. 1. Comparison of ROC curves for the QMKL – SVM and Gradient Boosting models on the DYRK1A test set. I.

The superior performance of the QMKL model suggests that the combination of multiple quantum kernels and a classical kernel was able to capture more complex, non-linear relationships within the data's feature space than the Gradient Boosting algorithm alone. While the computational cost of simulating quantum kernels is currently a limitation, these results strongly support the potential for quantum machine learning to provide a tangible advantage in real-world scientific applications.

V. CONCLUSION

In this work, we successfully developed and benchmarked a complete pipeline for a QSAR classification task, demonstrating that a quantum-enhanced model can outperform a strong classical baseline. Our QMKL – SVM approach, which combines quantum and classical kernels, achieved a higher AUC score than a tuned Gradient Boosting model on the DYRK1A inhibitor dataset.

The workflow, from SMILES conversion with RDKit to dimensionality reduction with PCA and finally to classification with a quantum-enhanced SVM, represents a viable and powerful strategy for applying QML to drug discovery. The results indicate that by mapping data into quantum Hilbert spaces, we can unlock new predictive capabilities. As quantum hardware continues to mature, fully leveraging the power of these quantum kernel methods will become increasingly feasible, positioning QMKL as a valuable and impactful tool for the future of computational chemistry and pharmacology.

It is important to highlight in this landscape that further investigations are required on how to represent and leverage descriptors in additional dimensions to enhance the robustness and predictive power of QSAR models.

ACKNOWLEDGMENT

This work was supported by the project ECO – 20241014 QUORUM funded by the Ministerio de Ciencia, Innovación y Universidades, through CDTI. We gratefully acknowledge ProtoQSAR SL and the team led by Eva Serrano-Candelas, Laureano E. Carpio, and Rafael Gozalbes for their fundamental contribution in providing, curating, and validating the dataset used in this study.

For more information about this research, please refer to:

[Computational Modeling of DYRK1A Inhibitors as Potential Anti-Alzheimer Agents.](#)

REFERENCES

- [1] C. Hansch and T. Fujita, " ρ - σ - π analysis. a method for the correlation of biological activity and chemical structure," *Journal of the American Chemical Society*, vol. 86, no. 8, pp. 1616–1626, 1964. [Online]. Available: <https://doi.org/10.1021/ja01062a035>
- [2] L. E. Carpio, Y. Sanz, R. Gozalbes, and S. J. Barigye, "Computational strategies for the discovery of biological functions of health foods, nutraceuticals and cosmeceuticals: a review," *Molecular Diversity*, vol. 25, pp. 1425–1438, 2021. [Online]. Available: <https://doi.org/10.1007/S11030-021-10277-5>
- [3] A. Tropsha, "Best practices for qsar model development, validation, and exploitation," *Molecular Informatics*, vol. 29, pp. 476–488, 2010. [Online]. Available: <https://doi.org/10.1002/MINF.201000061>
- [4] E. Serrano-Candelas, L. E. Carpio, and R. Gozalbes, "Computational modeling of dyrk1a inhibitors as potential anti-alzheimer agents," in *Computational Modeling of Drugs Against Alzheimer's Disease*, ser. Neuromethods, K. Roy, Ed. New York, NY: Springer US, 2023, vol. 203, pp. 295–324. [Online]. Available: https://doi.org/10.1007/978-1-0716-3311-3_10
- [5] R. R. Neubig, "International union of pharmacology committee on receptor nomenclature and drug classification. xxxviii. update on terms and symbols in quantitative pharmacology," *Pharmacological Reviews*, vol. 55, no. 4, pp. 597–606, 2003. [Online]. Available: <https://doi.org/10.1124/pr.55.4.4>
- [6] M. Schuld and N. Killoran, "Is quantum advantage the right goal for quantum machine learning?" *PRX Quantum*, vol. 3, no. 3, p. 030101, 2022. [Online]. Available: <https://link.aps.org/doi/10.1103/PRXQuantum.3.030101>
- [7] T. Suzuki, T. Hasebe, and T. Miyazaki, "Quantum support vector machines for classification and regression on a trapped-ion quantum computer," 2023. [Online]. Available: <https://arxiv.org/abs/2307.02091>
- [8] R. Natarajan, G. S. Natarajan, and S. C. Basak, "Quantitative structure–activity relationship (QSAR) modeling of chiral CCR2 antagonists with a multidimensional space of novel chirality descriptors," *Molecules*, vol. 30, no. 2, p. 307, 2025. [Online]. Available: <https://doi.org/10.3390/molecules30020307>
- [9] V. Svetnik, A. Liaw, C. Tong, J. C. Culberson, R. P. Sheridan, and B. P. Feuston, "Random forest: A classification and regression tool for compound classification and qsar modeling," *Journal of Chemical Information and Computer Sciences*, vol. 43, no. 6, pp. 1947–1958, 2003.
- [10] Ajay, W. P. Walters, and M. A. Murcko, "Can we learn to distinguish between drug-like and nondrug-like molecules?" *Journal of Medicinal Chemistry*, vol. 41, no. 18, pp. 3314–3324, 1998.
- [11] K.-C. Chen, X. Xu, H. Makhanov, H.-H. Chung, and C.-Y. Liu, "Quantum-enhanced support vector machine for large-scale stellar classification with GPU acceleration," 2023. [Online]. Available: <https://arxiv.org/abs/2311.12328>
- [12] V. Havlíček, A. D. Córcoles, K. Temme, A. W. Harrow, A. Kandala, J. M. Chow, and J. M. Gambetta, "Supervised learning with quantum-enhanced feature spaces," *Nature*, vol. 567, no. 7747, pp. 209–212, 2019. [Online]. Available: <https://doi.org/10.1038/s41586-019-0980-2>
- [13] S. Miyabe, B. Quanz, N. Shimada, A. Mitra, T. Yamamoto, V. Rastunkov, D. Alevras, M. Metcalf, D. J. M. King, M. Mamouei, M. D. Jackson, M. Brown, P. Intallura, and J.-E. Park, "Quantum multiple kernel learning in financial classification tasks," 2023. [Online]. Available: <https://arxiv.org/abs/2312.00260>
- [14] A. Gaulton *et al.*, "The ChEMBL database in 2023: a drug discovery platform spanning multiple bioactivity data types and time periods," *Nucleic Acids Research*, 2023.
- [15] G. V. W. Johnson and W. H. Stoothoff, "Tau phosphorylation in neuronal cell function and dysfunction," *Journal of Cell Science*, vol. 117, no. 24, pp. 5721–5729, 2004. [Online]. Available: <https://doi.org/10.1242/jcs.01558>
- [16] S. H. Bertz, "The first general index of molecular complexity," *Journal of the American Chemical Society*, vol. 103, no. 12, pp. 3599–3601, 1981. [Online]. Available: <https://doi.org/10.1021/ja00402a071>
- [17] P. Rebentrost, M. Mohseni, and S. Lloyd, "Quantum support vector machine for big data classification," *Physical Review Letters*, vol. 113, no. 13, p. 130503, 2014. [Online]. Available: <https://link.aps.org/doi/10.1103/PhysRevLett.113.130503>
- [18] H.-Y. Huang, M. Broughton, M. Mohseni, R. Babbush, S. Boixo, H. Neven, and J. R. McClean, "Power of data in quantum machine learning," *Nature Communications*, vol. 12, no. 1, p. 2508, 2021. [Online]. Available: <https://doi.org/10.1038/s41467-021-22539-9>
- [19] V. Bergholm, J. Izaac, M. Schuld, C. Gogolin, C. Blank, K. McKiernan, N. Killoran *et al.*, "PennyLane: Automatic differentiation of hybrid quantum-classical computations," *arXiv preprint arXiv:1811.04968*, 2018. [Online]. Available: <https://arxiv.org/abs/1811.04968>